CALCULATION OF ELECTRIC ARC INTERACTION WITH A TURBULENT GAS FLOW

N. A. Rubtsov and N. M. Ogurechnikova

UDC 535.2:533.9:15

The characteristics of an electric arc in a turbulent gas flow are studied. Relationships for calculating turbulent transport are presented.

In [1] the present authors studied the effect of radiation on turbulent energy transport in an electric arc. It was then assumed that the turbulence was of a hydrodynamic character and that the turbulence model of [2] could be used to complete the basic system of equations, without consideration of the presence of the electric arc in the gas flow.

In an electric arc with longitudinal draft, the turbulence is determined by the gas flow regime as well as volume heat liberation.

In the present study in calculating the characteristics of an arc in a turbulent gas flow, a turbulence model will be used which considers pulsations in radiation and electrodynamic quantities. An electric arc with longitudinal draft in a cylindrical channel will be considered.

The system of equations describing flow and heat exchange in the channel, averaged over time, has the form

$$\frac{\partial}{\partial x}(r\rho u)+\frac{\partial}{\partial r}(r\rho v)=0,$$

$$\rho u\frac{\partial u}{\partial x}+\rho v\frac{\partial u}{\partial r}=-\frac{\partial P}{\partial x}+\frac{1}{r}\frac{\partial}{\partial r}\left[r\mu\left(1+\frac{\nu_{\text{т}}}{\nu}\right)\frac{\partial u}{\partial r}\right],$$

$$\rho u c_p\frac{\partial T}{\partial x}+\rho v c_p\frac{\partial T}{\partial r}=\frac{1}{r}\frac{\partial}{\partial r}\left[r\lambda\left(1+\frac{\Pr}{\Pr_{\text{т}}}\frac{\nu_{\text{т}}}{\nu}\right)\frac{\partial T}{\partial r}\right]+$$

$$+u\frac{\partial P}{\partial x}+\mu\left(1+\frac{\nu_{\text{т}}}{\nu}\right)\left(\frac{\partial u}{\partial r}\right)^2+\sigma E^2\left[1+2\frac{\overline{\sigma' E'}}{\sigma E}+\frac{\overline{E'^2}}{E^2}\right]-\operatorname{div} q_r,$$

$$j=\sigma E+\overline{\sigma' E'},$$

$$G=2\pi\int_0^R\rho u r dr$$

with boundary conditions

$$x=0,\ 0\leqslant r\leqslant R,\ T=T_{\text{в}}(r),\ u=u_{\text{в}}(r);$$

$$x>0,\ r=0,\ dT/dr=0,\ du/dr=0,\ v=0;$$

$$r=R,\ T=T_{\text{w}},\ u=0,\ v=0.$$

Turbulence characteristics are determined by the equation of temperature pulsation intensity. Relying on the existence of an "equilibrium" turbulence structure [2] and considering the interaction of temperature pulsations with pulsations in the electrodynamic quantities, the equation for temperature pulsation intensity can be written in the following form:

$$\overline{v'T'}\frac{\partial T}{\partial r}-\frac{2}{\rho c_p}\sigma E\overline{E'T'}-\frac{E^2}{c_p\rho}\overline{\sigma' T'}=a\overline{\frac{\partial T'}{\partial r}\frac{\partial T'}{\partial r}}+\frac{1}{c_p\rho}\overline{T'\operatorname{div} q_r'}. \quad (1)$$

Using relationships describing correlations of the electrodynamic quantity pulsations [3-4]

Thermophysics Institute, Siberian Branch, Academy of Sciences of the USSR, Novosibirsk.
Translated from Inzhenerno-Fizicheskii Zhurnal, Vol. 54, No. 4, pp. 550-557, April, 1988. Original article submitted November 11, 1986.

0022-0841/88/5404-0373$12.50

$$\overline{E'T'} = -\frac{1}{3} E' g \overline{T'^2},$$

$$\overline{\sigma' E'} = -\frac{1}{3} \sigma(T) E g^2 \overline{T'^2},$$

$$\overline{E'^2} = \frac{1}{3} \frac{\overline{\sigma'^2}}{\sigma^2} E^2,$$

$$g = d \ln \sigma(T)/dt$$

and transforming Eq. (1) in accordance with [2], we arrive at

$$\frac{K_2^2 \omega^2}{a_T} \overline{T'^2} = A_2 \left(a + \beta a_T + \frac{f l^2}{\beta A_2} \right) \frac{\overline{T'^2}}{l^2} + \frac{\sigma E^2 g \overline{T'^2}}{3 c_p \rho}, \tag{2}$$

in which

$$\omega^2 = \nu_t \tau / \rho K_1 (\nu + \nu_t). \tag{3}$$

Here

$$\frac{1}{c_p \rho} \overline{T' \operatorname{div} q_r'} = f \overline{T'^2}.$$

The expression for the turbulent Prandtl number can be obtained from Eq. (2) in the following form:

$$\mathrm{Pr}_t = \{\nu_T/\nu\} \left\{ -\frac{1}{2\beta \mathrm{Pr}_{ef}} \left(1 + \frac{l^2}{3A_2} \frac{\sigma E^2 g}{\lambda} \right) + \right.$$
$$\left. + \sqrt{\left(\frac{1}{2\beta \mathrm{Pr}_{ef}} \right)^2 \left(1 + \frac{l^2}{3A_2} \frac{\sigma E^2 g}{\lambda} \right) + \frac{1}{\overline{\mathrm{Pr}_T^2}} \frac{\nu_T}{\nu} \left(\frac{\nu_T}{\nu} + \frac{1}{\alpha} \right)} \right\}^{-1}, \tag{4}$$

where $\mathrm{Pr}_{ef} = \mathrm{Pr}/(1 + \gamma)$, $\gamma = f l^2/A_2 \rho$, the empirical constants $\overline{\mathrm{Pr}}_t = \sqrt{\beta K_1 A_2}/K_2$, A_2, β, α are taken in accordance with [2].

The turbulent viscosity coefficient is defined by the relationships of Reichardt [5] and Deissler [6]. The turbulence scale is found from the Prandtl–Nikuradze expression.

The mean electrical conductivity is calculated in terms of the temperature pulsations [7]:

$$\sigma = \frac{\sigma(T)}{1 + \frac{\nu_{ea}}{\nu_g} \left[\exp\left(\frac{\varkappa^2}{2} \right) - 1 \right]},$$

and thus the electric field intensity is defined by the expression

$$E = \frac{j}{\sigma} \left\{ 1 + \frac{\nu_{ea}}{\nu_g} \left[\exp\left(\frac{\varkappa^2}{2} \right) - 1 \right] \right\},$$

where

$$\varkappa = \frac{E_i}{2kT} \frac{\sqrt{\overline{T'^2}}}{T}, \quad \nu_g = \nu_{ei} + \nu_{ea}.$$

With consideration of volume heat liberation, the mean square temperature pulsations are found from Eqs. (2), (3):

$$\overline{T'^2} = l^2 \left(\frac{\partial T}{\partial r} \right)^2 \frac{a_T/\nu}{A_2 \beta \left(\frac{1}{\beta \mathrm{Pr}_{ef}} + \frac{a_T}{\nu} \right) + \frac{l^2}{3\lambda} \frac{\sigma E^2 g}{\mathrm{Pr}_{ef}}}. \tag{5}$$

In electric arc heaters in the initial and transitional segments radiant heat exchange is significant. Here there are large axial temperature gradients, and therefore energy transport by radiation will be considered two-dimensional.

Assuming that the gas radiates and absorbs (scattering will not be considered), the divergence of the radiant heat flux can be written in the following manner:

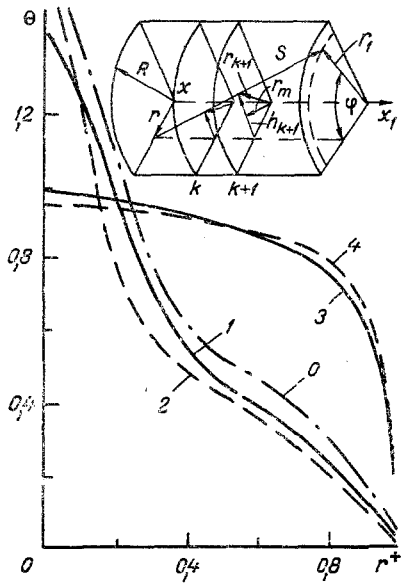

Fig. 1. Development of radial temperature distributions $\Theta = T/T_0$ over channel length: 0, 1, 2, 3, 4) zeroth approximation without radiation; 0.005, 0.005 (without radiation), 0.1, 0.4 m; $r^+ = r/R$, $R = 0.5 \cdot 10^{-2}$ m; I = 250 A; G = 3 g/sec, T_0 = 11,686 K.

$$-\operatorname{div} q_r = -\operatorname{div}\left(\int_0^\infty \int_0^{4\pi} I_\nu d\Omega d\nu\right) = \int_0^\infty \int_0^{4\pi} \frac{dI_\nu}{dS} d\Omega d\nu, \tag{6}$$

where I_ν is defined by the formal solution of the radiation transport equation

$$I_\nu = J_\nu \exp\left[-\tau(S_w)\right] + \int_0^{S_w} \chi_\nu B_\nu \exp\left[-\tau(S)\right] dS. \tag{7}$$

Using Eqs. (7) and (8) the expression for the divergence of the radiant heat flux can be brought to the form

$$\begin{aligned} -\operatorname{div} q_r = \int_0^\infty \chi_\nu \int_0^{2\pi} (I_\nu - B_\nu)\, d\Omega d\nu \quad = \int_0^\infty \left\{ \chi_\nu \int_0^{4\pi} J_\nu \exp\left[-\tau(S_{ст})\right] d\Omega + \right. \\ \left. + \chi_\nu \int_0^{4\pi} \int_0^{S_w} \chi_\nu B_\nu \exp\left[-\tau(S)\right] dS d\Omega - 4\pi \chi_\nu B_\nu \right\} d\nu. \end{aligned} \tag{8}$$

We will consider radiation transport in a finite cylinder (Fig. 1). As in the figure, the arc length S is defined as

$$S = \left[(x - x_1)^2 + r^2 + r_1^2 + 2 r r_1 \cos\varphi\right]^{1/2}.$$

In a cylindrical coordinate system Eq. (8) takes on the form

$$\begin{aligned} \operatorname{div} q_r = \int_0^\infty \left\{ 4\pi \chi_\nu B_\nu - \chi_\nu \int_{-\infty}^\infty \int_0^R \chi_\nu B_\nu r_1 \int_0^{2\pi} \exp\left[-\tau(S)\right] d\varphi dr_1 \frac{dx}{S^2} - \right. \\ \left. - \chi_\nu \int_{-\infty}^\infty J_\nu(x) \int_0^{2\pi} \exp\left[-\tau(S_{ст})\right] (R - r\cos\varphi)\, R \frac{d\varphi dx}{S_w^3} \right\} d\nu, \end{aligned} \tag{9}$$

where

$$\tau(S) = \int_0^S \chi_\nu(S)\, dS.$$

Considering Fig. 1, we transform the expression for optical path length to the form

$$\tau = \int_0^x \frac{\chi_\nu(x)\, x dx}{\sqrt{x^2 + r^2 + r_1^2 - 2 r r_1 \cos\varphi}} + \left[2K \int_{r_m}^m F(r')\, dr' + \int_m^n F(r')\, dr'\right],$$

where

$$F(r') = \chi_\nu r'/\sqrt{x^2 + r'^2 + r_m^2},$$

$$m = r_1,\ n = r,\ r_1 < r;$$

$$m = r,\ n = r_1,\ r < r_1;$$

$$K = \begin{cases} 0 & \text{at} \quad \cos\varphi \geqslant m/n \\ 1 & \text{at} \quad \cos\varphi < m/n. \end{cases}$$

We calculate the radiant heat-exchange layer by layer. For a layer Eq. (9) is written in the following form:

$$\begin{aligned} \operatorname{div} q_r = \int_0^\infty \Bigg\{ & 4\pi\chi_\nu B_\nu - \chi_\nu \int_{x_k}^{x_{k+1}} \int_0^R \chi_\nu B_\nu r_1 \int_0^{2\pi} \exp\left[-\tau(S)\right] d\varphi dr_1 \frac{dx}{S^2} - \\ & - \Bigg\{ \int_0^{x_k} \left[4\pi\chi_\nu B_\nu - \chi_\nu \int_0^R \chi_\nu B_\nu r_1 \int_0^{2\pi} \exp\left[-\tau(S)\right] d\varphi dr_1 \frac{1}{S^2} \right] dx + \\ & + \int_{k+1}^{l} \left[4\pi\chi_\nu B_\nu - \chi_\nu \int_0^R \chi_\nu B_\nu r_1 \int_0^{2\pi} \exp\left[-\tau(S)\right] d\varphi dr_1 \frac{1}{S^2} \right] dx \Bigg\} \int_{x_k}^{x_{k+1}} \int_0^R \int_0^{2\pi} \exp\left[-\tau(S)\right] d\varphi dr_1 \frac{dx}{S^2} + \\ & + \int_{x_k}^{x_{k+1}} J_\nu(x) \int_0^{2\pi} \exp\left[-\tau(S_w)\right](R - r\cos\varphi) R \frac{d\varphi dx}{S_w^3} \Bigg\} d\nu. \end{aligned} \tag{10}$$

The radiant heat flux on the wall is determined from the radial flux component

$$q_r = \int_0^\infty \int_0^{2\pi} I_\nu \cos(r,\ S)\, d\Omega d\nu.$$

Following [8], we divide the radiant flux into two components: $q_r = q_r^+ - q_r^-$. For the geometry considered, the radiant flux components on the wall are equal to

$$\begin{aligned} q_r^+ = \int_0^\infty \Bigg\{ & \int_{-\infty}^{\infty} J_\nu \int_0^{2\pi} \exp\left[-\tau(S_w)\right](R - R\cos\varphi)^2 R d\varphi \frac{dx}{S_w^4} + \\ & + \int_{-\infty}^{\infty} \int_0^R \chi_\nu B_\nu r_1 \int_0^{2\pi} \exp\left[-\tau(S)\right](R - r_1\cos\varphi)\, d\varphi dr_1 \frac{dx}{S^3} \Bigg\} d\nu, \end{aligned} \tag{11}$$

$$q_r^- = \pi \int_0^\infty J_\nu d\nu. \tag{12}$$

For a layer Eq. (11) can be written as

$$\begin{aligned} q_r^+ = \int_0^\infty \Bigg\{ & \int_{x_k}^{x_{k+1}} J_\nu \int_0^{2\pi} \exp\left[-\tau(S_w)\right](R - R\cos\varphi)^2 R d\varphi \frac{dx}{S_w^4} + \\ & + \int_{x_k}^{x_{k+1}} \int_0^R \chi_\nu B_\nu r_1 \int_0^{2\pi} \exp\left[-\tau(S)\right](R - r_1\cos\varphi)\, d\varphi dr_1 \frac{dx}{S^3} + \\ & + \Bigg[\int_0^{x_k} \int_0^R \chi_\nu B_\nu r_1 \int_0^{2\pi} \exp\left[-\tau(S)\right](R - r_1\cos\varphi)\, d\varphi dr_1 \frac{dx}{S^3} + \\ & + \int_{x_{k+1}}^{l} \int_0^R \chi_\nu B_\nu r_1 \int_0^{2\pi} \exp\left[-\tau(S)\right](R - r_1\cos\varphi)\, d\varphi dr_1 \frac{dx}{S^3} \Bigg] \times \\ & \times \int_{x_k}^{x_{k+1}} \int_0^R \int_0^{2\pi} \exp\left[-\tau(S)\right](R - r_1\cos\varphi)\, d\varphi dr_1 \frac{dx}{S^3} \Bigg\} d\nu. \end{aligned} \tag{13}$$

The system of equations was solved by the finite-difference method. The energy and motion equations were approximated by an implicit difference method, and the continuity equation, by an explicit one. A grid nonuniform in the radial direction was chosen. The pressure gradient was determined by a splitting method. The system of difference equations was solved by the iteration method in combination with the drive method.

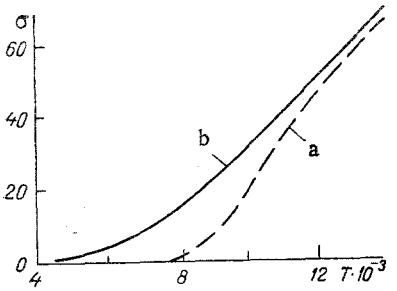

Fig. 2

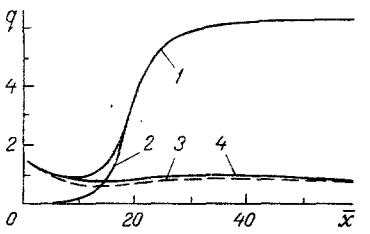

Fig. 3

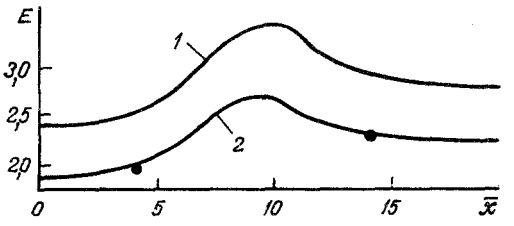

Fig. 4

Fig. 2. Electrical conductivity coefficient S/m vs temperature, K: a, b) turbulent and laminar flows

Fig. 3. Thermal flux distributions on wall, MW/m^2, over channel length: 1, 2, 3, 4) total, conductive, radiant, radiant (two-dimensional) fluxes. $R = 0.5 \cdot 10^{-2}$ m, I = 250 A, G = 3 g/sec; $\bar{x} = x/2R$.

Fig. 4. Electric field intensity distribution, V/m, over channel length: 1, 2) with and without consideration of temperature pulsations; points) experiment [9]; $R = 1.5 \cdot 10^{-2}$ m, I = 100 A, G = 8 g/sec.

In calculating the radiant flux divergence in the k-th layer, the temperature distribution in the k + 1...M layers were unknown, so the temperature field in layers 1 − M was calculated without consideration of radiation.

Studies were performed for an arc with a turbulent draft of argon in a cylindrical channel.

The Reynolds numbers, defined from the mean mass gas flow rate through a unit area of the channel section at the temperature of the wall, were equal to $Re > 8 \cdot 10^3$ in a channel $1 \cdot 10^{-2}$ m in diameter, 0.6 m long, at a current of 250 A, flow rate of 3 g/sec, and $Re > 6 \cdot 10^3$ in a channel $3 \cdot 10^{-2}$ m in diameter at a current of 100 A and flow rate of 8 g/sec.

The calculations performed showed that the temperature (Fig. 1) changes more markedly in the initial segment, where the role of turbulent heat transport and reabsorption of radiation increases.

The dependence of mean values of the electrical conductivity coefficient in the turbulent argon flow upon temperature is shown in Fig. 2, and compared to values of the same coefficient in a laminar flow. Electrical conductivity in the turbulent flow was calculated with consideration of temperature pulsations. The values of the electrical conductivity coefficient in the turbulent flow are lower than those in the laminar. The greatest reduction occurs at a temperature of 9000 K.

Calculated thermal flux values are shown in Fig. 3. In the initial portion of the channel the basic contribution to thermal flux is produced by radiation. The radiant flux decreases over channel length. For two-dimensional radiation transport the radiant flux on the wall (solid curve) is greater than the one-dimensional. The deviation is about 10% for a temperature of 13,000 K, but for certain regimes in high intensity arcs it may be significantly higher. In the initial segment where the conductive flux is less than the radiant, there is a minimum in total thermal flux. In the transition segment the growth of molecular and turbulent thermal conductivity leads to a significant increase in both conductive and total flux, while the radiant component has a minimum and is almost constant in the segment

of developed turbulent motion. The reduction in radiant flux in the transition segment can be explained by the effect of radiation on turbulent energy transport. The conductive flux in the developed turbulent segment increases insignificantly, its value being attributable to the change in the value of the temperature gradient at the wall.

It was noted in [9] that a growth in electric field intensity in argon arcs is observed in channels with diameter $d > 2 \cdot 10^{-2}$ m. Results of a calculation of electric field intensity over channel length are shown in Fig. 4. Studies were performed for a channel $3 \cdot 10^{-2}$ m in diameter. The intensity values calculated with consideration of temperature pulsations were 20% above the values for a laminar arc. In the transition segment, after reaching a maximum value, the field intensity decreases. The calculations show that this reduction reaches 14% upon approach to the stabilized segment. The reduction in intensity corresponds to a decrease in turbulent heat transport.

In view of the absence of data describing turbulent arc structure, the only method for determining the reliability of the proposed model is comparison of calculated data to experiment. Figure 4 shows experimental data of [9], obtained for a twisted flow. The twisting reduces electric field intensity. The agreement between experiment and calculated data on intensity with consideration of temperature pulsations proves to be better without consideration of twisting.

NOTATION

T, temperature; λ, σ, ρ, c_p, thermal conductivity, electrical conductivity, density, specific heat at constant pressure; P, pressure; u, v, longitudinal and transverse velocity components; μ, dynamic viscosity; ν, ν_t, molecular and turbulent kinematic viscosities; I, current; E, electric field intensity; G, gas flow rate; a, a_t, molecular and turbulent thermal diffusivity; ℓ, turbulence scale, channel length; E_i, ionization potential; ν_{ea}, ν_{ei}, electron–atom and electron–ion collision frequencies; τ, optical path length, shear stress; I_ν, J_ν, spectral intensity of gas and wall radiation; B_ν, spectral intensity of equilibrium radiation; χ_ν, spectral absorption coefficient; Ω, solid angle; x, r, φ, coordinates; R, channel radius. Subscripts: i, at input; w, wall; ', pulsation value.

LITERATURE CITED

1. N. A. Rubtsov and N. M. Ogurechnikova, Teplofiz. Vys. Temp., 21, No. 6, 1134-1138 (1983).
2. V. M. Ievlev, Turbulent Motion of High Temperature Continuous Media [in Russian], Moscow (1975).
3. V. I. Artemov, A. B. Vatazhin, Yu. S. Levitan, and O. A. Sinkevich, 9th All-Union Conference on Low Temperature Plasma Generators: Papers [in Russian], Frunze (1983), pp. 62-63.
4. B. A. Uryukov, Izv. Sib. Otd. Akad. Nauk SSSR, Ser. Tekh. Nauk, No. 1, 87-98 (1981).
5. Reichardt, Z. Angew. Math. Mech., 31, No. 7, 208-219 (1951).
6. R. G. Deissler, NASA TR, No. 1210 (1955).
7. I. P. Shkarofsky, ARL, No. 73-0133 (1973).
8. M. A. Heaslet and R. F. Warming, JQSRT, 6, No. 6, 751-774 (1966).
9. G. Yu. Dautov and M. I. Sazonov, Low Temperature Plasma Generators: Proc. 3rd All-Union Scientific-Technical Conference on Low Temperature Plasma Generators [in Russian], Moscow (1969), pp. 200-208.